

Local structures of mechanically alloyed Fe_{100-x}Cu_x solid solutions studied by X-ray absorption fine structure

Shiqiang Wei^a, Wensheng Yan^a, Jiangwei Fan^a, Yuzhi Li^b, and Wenhan Liu^b, and Xiaoguang Wang^a

^aNational Synchrotron Radiation Laboratory, University of Science & Technology of China, Hefei, 230029, P. R. China, ^bCenter of Physics and Chemistry, and Department of Physics, University of Science & Technology of China, Hefei, 230026, P. R. China, E-mail: sqwei@ustc.edu.cn

The local structures of the immiscible Fe_{100-x}Cu_x alloys ($x = 0, 10, 20, 40, 60, 80$ and 100) produced by mechanical alloying have been investigated by XAFS. For the Fe_{100-x}Cu_x ($x \geq 40$) solid solutions, the local structures around Fe atoms change from bcc structure to fcc one and the Cu atoms maintain the original coordination geometry after milling for 160 hours. On the contrary, the local structures around Cu atoms in both of Fe₈₀Cu₂₀ and Fe₉₀Cu₁₀ alloys appear a transition from fcc to bcc structure. We found that the Debye-waller factor σ of fcc Fe-Cu phase is larger than that of bcc Fe-Cu phase, and the σ (0.099 \AA) around Fe atoms is larger than that (0.089 \AA) of Cu in the Fe_{100-x}Cu_x ($x \geq 40$) solid solutions. This suggests that the mechanically alloyed Fe_{100-x}Cu_x supersaturated solid solution is not a homogeneous alloy, and consists of Fe-rich and Cu-rich regions for various compositions. A possible mechanism for bcc-to-fcc and fcc-to-bcc changes in Fe_{100-x}Cu_x solid solutions is discussed in relation to the interdiffusion and transition induced by the ball milling.

Keywords: XAFS, Fe_{100-x}Cu_x solid solution, mechanical alloying.

1. Introduction

Recently, mechanical alloying (MA) has been attracted much attention in the fields synthesizing amorphous alloy, intermetallic compounds and solid solutions (Huang *et al.*, 1998; Schultz *et al.*, 1988; Koch *et al.*, 1983). In particular, MA can drive binary or ternary immiscible system with positive heat of mixing to form supersaturated solid solutions which are never obtained with normal metallurgic and quenching method, *i.e.* Fe-Cu, Cu-Ta, Cu-V, Cu-Ag, Cu-W binary metals (Shigu *et al.*, 1990; Fukunaga *et al.*, 1991; Gaffet *et al.*, 1991; Sakurai *et al.*, 1990). The mechanically alloyed Fe_{100-x}Cu_x solid solution is an interesting system due to its electronic and magnetic properties depending on the composition. Therefore, the solid solubility and structure of Fe_{100-x}Cu_x have been widely investigated by Uenishi and Shingu *et al.* (1990,1992), Yavari *et al.* (1992), Crespo *et al.* (1993, 1994), Huang *et al.* (1996, 1998), Shilling *et al.* (1996, 1990) and Wei *et al.* (1994, 1997) with differential scanning calorimetry (DSC), x-ray diffraction (XRD), transmission electron microscopy (TEM), Mossbauer spectroscopy and x-ray absorption fine structure (XAFS) techniques. On the basis of the results mentioned above, it has been concluded that alloying at atomic level occurs in the Fe_{100-x}Cu_x system during milling process. It is found that a single-phase fcc solid solution is

obtained for $x > 40$, and bcc solid solution is obtained on the Fe-rich side for $x < 20$, and two phase region with coexisting fcc and bcc solution for $20 < x < 40$. However, the mechanism responsible for significantly enhanced solubility is still a subject of debate.

In this paper, XAFS has been performed to measure the local structure evolutions of Fe and Cu atoms in Fe_{100-x}Cu_x with the atomic concentration of x value in a large composition range. We aimed at studying the local structure around Fe and Cu atoms: to clarify the effect of the ball milling and investigate whether immiscible Fe and Cu atoms form a uniformly supersaturated solid solution alloy or not.

2. Experiment

Crystalline iron and copper powders with purity higher than 99.9% and with particle sizes less than $20 \mu\text{m}$ were mixed to the desired composition Fe_{100-x}Cu_x ($x = 0, 10, 20, 40, 60, 80, 100$). The mixture and tungsten carbide balls were sealed inside a cylindrical stainless steel vial filled with argon gas. The weight ratio of the ball to powder is 10 to 1. MA was performed in a planetary ball with a rotation speed of about 210 r/min. The samples of Fe_{100-x}Cu_x were obtained after Fe_{100-x}Cu_x mixtures were milled for 160 hours.

The x-ray absorption spectra of Fe_xCu_{100-x} samples at Fe and Cu K-edge were measured at the beamline of U7C of National Synchrotron Radiation Laboratory (NSRL) and the beamline of 4W1B of Beijing Synchrotron Radiation Facility (BSRF). The storage ring of NSRL was operated at 0.8 GeV with a maximum current of 160 mA, The storage ring of BSRF was run at 2.2 GeV with a maximum current of 100 mA. The fixed-exit Si(111) flat double crystals were used as monochromator. The XAFS spectra were recorded in transmission mode with ionization chambers filled with Ar/N₂ at room temperature. XAFS Data were analyzed by USTCXAFS1 soft package compiled by Wan and Wei and UWXAFS3.0 software package according to the standard procedures (Wan and Wei, 1999; Stern *et al.*, 1995; Sayers *et al.*, 1988).

3. Results and Discussions

The Fourier transform (FT) of the EXAFS oscillation function $k^3\chi(k)$ at Fe K-edge is shown in Fig. 1(a) for mechanically alloyed Fe_{100-x}Cu_x solid solutions. A strong peak around 2.2 \AA is the first nearest neighbor coordination shell. The magnitude intensity of the third peak ($R=4.48 \text{ \AA}$), which is sensitive to the coordination geometry, is not observed in the FT for Fe_{100-x}Cu_x ($x \geq 40$). In contrast, it is clear that the FT of the Fe K-EXAFS for Fe₆₀Cu₄₀ becomes similar to that of Cu K-EXAFS for metal Cu in Fig. 1(b). The FT of Fe K-EXAFS for Fe₆₀Cu₄₀ shows that the mechanical alloying changes the local structure of Fe atoms from a bcc-like structure to a fcc-like one. The FT results of Fe K-EXAFS for Fe₈₀Cu₂₀ and Fe₉₀Cu₁₀ suggest that after 160 hour milling, the local structure of Fe atom remains to be a bcc-like structure, and the FT of Cu K-EXAFS changes from a fcc-like structure to a bcc-like one. Using the amplitude $|F(k,p)|$ and phase shift $f(k)$ of standard samples obtained from the bcc α -Fe and fcc metal Cu, *i.e.* Fe₅₀Cu₅₀ powder mixture, and FEFF7 (Rehr *et al.*, 1992), the curve fitting was performed (Sayers *et al.*, 1988). The results are summarized in Table 1 and Table 2.

In order to study the local structural evolutions of Fe_{100-x}Cu_x solid solution during the MA process, a series of Fe_{100-x}Cu_x ($x=0, 10, 20, 40, 60, 70, 80, 100$) samples with various compositions were selected for investigation. The EXAFS results in Fig.1 show that the radial distribution functions (RDF) of Fe_{100-x}Cu_x solid

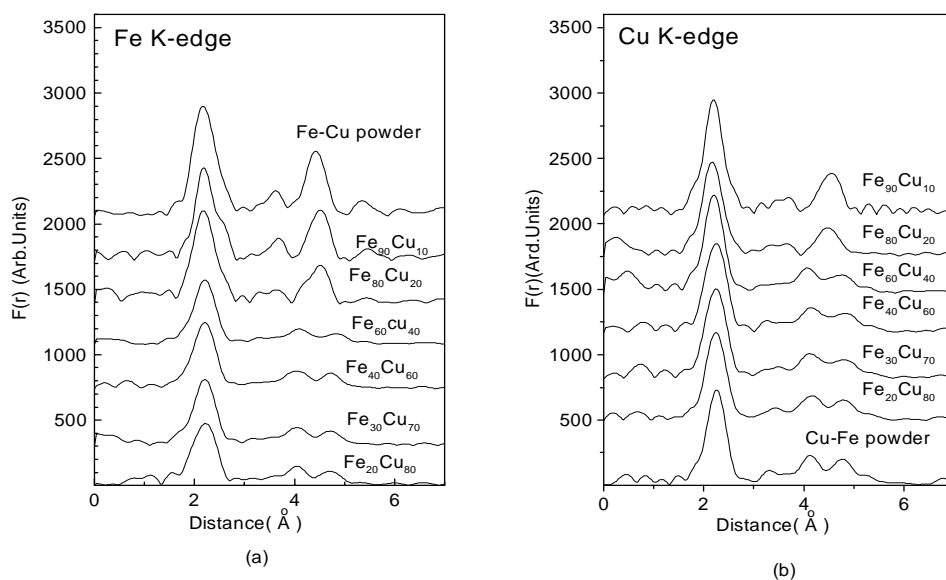


Figure.1
Radial distribution functions for the MA $\text{Fe}_{100-x}\text{Cu}_x$, Fe K-edge (a), Cu K-edge (b).

Table 1

The structural parameters of $\text{Fe}_{100-x}\text{Cu}_x$ solid solutions fitting for Fe K-edge EXAFS spectra

Sample	Bond type	R(Å)	$\sigma(\text{Å})$	N	ΔE_0
Fe powder	Fe-Fe	2.48 ± 0.01	0.070 ± 0.005	8.0 ± 0.5	2.97
	Fe-Fe	2.85 ± 0.01	0.075 ± 0.005	6.0 ± 0.5	5.0
$\text{Fe}_{90}\text{Cu}_{10}$	Fe-Fe	2.48 ± 0.01	0.078 ± 0.005	8.0 ± 0.5	-4.01
	Fe-Cu	2.48 ± 0.01	0.080 ± 0.005	0.5 ± 0.2	-1.59
	Fe-M	2.85 ± 0.01	0.081 ± 0.005	5.5 ± 0.5	5.0
$\text{Fe}_{80}\text{Cu}_{20}$	Fe-Fe	2.48 ± 0.01	0.081 ± 0.005	7.4 ± 0.5	-2.01
	Fe-Cu	2.49 ± 0.01	0.081 ± 0.005	1.2 ± 0.2	7.31
	Fe-M	2.85 ± 0.01	0.081 ± 0.005	5.3 ± 0.5	5.0
$\text{Fe}_{60}\text{Cu}_{40}$	Fe-Fe	2.57 ± 0.01	0.099 ± 0.005	8.7 ± 0.5	0.64
	Fe-Cu	2.56 ± 0.01	0.099 ± 0.005	3.5 ± 0.3	-4.99
$\text{Fe}_{40}\text{Cu}_{60}$	Fe-Fe	2.58 ± 0.01	0.099 ± 0.005	6.9 ± 0.5	4.99
	Fe-Cu	2.58 ± 0.01	0.099 ± 0.005	5.6 ± 0.5	2.63
$\text{Fe}_{30}\text{Cu}_{70}$	Fe-Fe	2.58 ± 0.01	0.098 ± 0.005	5.7 ± 0.5	4.96
	Fe-Cu	2.58 ± 0.01	0.098 ± 0.005	6.4 ± 0.5	2.94
$\text{Fe}_{20}\text{Cu}_{80}$	Fe-Fe	2.58 ± 0.01	0.098 ± 0.005	5.0 ± 0.5	4.95
	Fe-Cu	2.58 ± 0.01	0.098 ± 0.005	7.1 ± 0.5	3.45

M = Fe, Cu

solutions still preserve the polycrystalline structure after MA process, since the magnitude peaks of the higher coordination shell appear. Our previous results have indicated that the MA can drive the $\text{Fe}_{100-x}\text{Cu}_x$ solid solutions into nanometer grains but it does not greatly destroy their crystalline structure. (Wei et al., 1997). For $\text{Fe}_{90}\text{Cu}_{10}$ and $\text{Fe}_{80}\text{Cu}_{20}$, the EXAFS results in Fig. 1 (a) and (b) demonstrate that the bcc-structure is maintained for Fe atoms but the fcc-structure Cu atoms change into a bcc-like one after milling, and the structural parameters in table 2 further illustrate that the bond distance ($R_{\text{Cu-Cu}} = 2.50 \text{ Å}$) and coordination number ($N = 8.1$) are 0.06 Å shorter and 4 smaller than those of the Cu powder, respectively. In addition, it can be noted that the magnitude of the prominent peak in the FT of Cu K-edge EXAFS

Table 2

The structural parameters of $\text{Fe}_{100-x}\text{Cu}_x$ solid solutions fitting for Cu K-edge EXAFS spectra

Sample	Bond type	R(Å)	$\sigma(\text{Å})$	N	ΔE_0
$\text{Fe}_{90}\text{Cu}_{10}$	Cu-Cu	2.48 ± 0.01	0.078 ± 0.005	2.0 ± 0.3	-3.1
	Cu-Fe	2.48 ± 0.01	0.073 ± 0.005	6.2 ± 0.5	-5.0
	Cu-M	2.84 ± 0.01	0.078 ± 0.005	5.8 ± 0.5	5.0
$\text{Fe}_{80}\text{Cu}_{20}$	Cu-Cu	2.50 ± 0.01	0.082 ± 0.005	3.1 ± 0.3	4.8
	Cu-Fe	2.49 ± 0.01	0.081 ± 0.005	5.0 ± 0.5	4.0
	Cu-M	2.87 ± 0.01	0.082 ± 0.005	5.5 ± 0.5	5.0
$\text{Fe}_{60}\text{Cu}_{40}$	Cu-Cu	2.55 ± 0.01	0.089 ± 0.005	7.1 ± 0.5	2.7
	Cu-Fe	2.55 ± 0.01	0.087 ± 0.005	4.6 ± 0.5	0.9
$\text{Fe}_{40}\text{Cu}_{60}$	Cu-Cu	2.56 ± 0.01	0.089 ± 0.005	8.4 ± 0.5	-3.9
	Cu-Fe	2.54 ± 0.01	0.089 ± 0.005	3.3 ± 0.3	-4.3
$\text{Fe}_{30}\text{Cu}_{70}$	Cu-Cu	2.55 ± 0.01	0.089 ± 0.005	9.7 ± 0.5	-1.8
	Cu-Fe	2.54 ± 0.01	0.089 ± 0.005	2.3 ± 0.3	-3.8
$\text{Fe}_{20}\text{Cu}_{80}$	Cu-Cu	2.55 ± 0.01	0.089 ± 0.005	9.8 ± 0.5	-2.1
	Cu-Fe	2.54 ± 0.01	0.088 ± 0.005	1.5 ± 0.3	-4.6
Cu powder	Cu-Cu	2.55 ± 0.01	0.089 ± 0.005	12.0 ± 0.5	0.4

increases by about 20% for the $\text{Fe}_{90}\text{Cu}_{10}$ and $\text{Fe}_{80}\text{Cu}_{20}$, compared with the intensity of Cu atoms in $\text{Fe}_{00-x}\text{Cu}_x$ ($x \geq 40$) solid solutions. The results indicate that the Cu atoms are incorporated into the bcc α -Fe phase for $\text{Fe}_{100-x}\text{Cu}_x$ samples ($x < 20$) by MA. That the local structures of Fe atoms of $\text{Fe}_{90}\text{Cu}_{10}$ and $\text{Fe}_{80}\text{Cu}_{20}$ do not change into fcc-like is possibly related to the fact that of Cu ratio (Cu < 20%).

For the $\text{Fe}_{00-x}\text{Cu}_x$ ($x \geq 40$) solid solutions, it was found that the intensity of the main peak in the FT of Cu K-EXAFS does not show a noticeable change (smaller than 10%) with the x value while the main peak intensity for the Fe K-EXAFS abruptly decreases by half. Moreover, the RDF intensity of Fe atoms is about 30% lower than that of Cu atoms in $\text{Fe}_{100-x}\text{Cu}_x$ ($x \geq 40$) solid solutions, despite the RDF intensity of Fe powder is slightly higher than that of Cu powder. This suggests that the MA can

drive the local structure around Cu atoms in samples ($x \geq 40$) to produce a smaller defect but the local structure of Fe atoms is seriously modified. The local neighbor environment around Fe atoms is evidently different from that of Cu atoms in a MA $\text{Fe}_{100-x}\text{Cu}_x$ solid solution. Hence, It can be concluded that the $\text{Fe}_{100-x}\text{Cu}_x$ supersaturated solid solution is an inhomogeneous alloy, and there are Fe-rich and Cu-rich regions in the MA $\text{Fe}_{100-x}\text{Cu}_x$ solid solutions. If the $\text{Fe}_{100-x}\text{Cu}_x$ solid solutions is a homogeneous alloy, the σ of Fe atoms should be nearly the same as that of Cu atoms in the $\text{Fe}_{100-x}\text{Cu}_x$ solid solutions with middle composition, i.e., $\text{Fe}_{60}\text{Cu}_{40}$ and $\text{Fe}_{40}\text{Cu}_{60}$ solid solutions. Furthermore, the σ of Fe atoms (0.099 Å) is larger than that (0.089 Å) of Cu atoms as shown in table 1 and 2 for $\text{Fe}_{100-x}\text{Cu}_x$ solid solutions ($x \geq 40$). On the other hand, The disorder degree σ in fcc Fe-Cu solid solution is larger than that in the bcc Fe-Cu one. It implies that the lattice of fcc Fe-Cu alloying phase is expected to have a large distortion, compared with that of bcc Fe-Cu one.

The previous results (Wei *et al.*, 1997) have revealed that a higher Cu concentration is favorable to make $\text{Fe}_{100-x}\text{Cu}_x$ solid solution to fine particles with TEM. Their average sizes are 350 and 150 Å for $\text{Fe}_{80}\text{Cu}_{20}$ and $\text{Fe}_{60}\text{Cu}_{40}$, respectively. From viewpoints of interface diffusion, the Cu atoms near the Fe grain boundary are easier to alloy into fcc phase. From viewpoints of internal pressure or stress, a smaller grain size is advantageous for phase change. Doyoma *et al.* (1991) and Keavney *et al.* (1995) reported that 11 layers of fcc-phase Fe could be epitaxially grown on the Cu (001) and $\text{Cu}_x\text{Au}_{1-x}$ single crystal. It was confirmed that the small size of Fe cluster could stably exist. In $\text{Fe}_{80}\text{Cu}_{20}$ solid solution where Fe particles do not form small size clusters, both Cu and Fe atoms have bcc-like medium-range order. In $\text{Fe}_{60}\text{Cu}_{40}$ solid solution, the local structure of Fe atoms gradually transits into a fcc structure from a bcc one as the particle size becomes very small. Huang *et al.* (1998) and Wei *et al.* (1997) have considered that Cu atoms can induce the smaller Fe particle to produce a structural transition from a bcc structure to a fcc one.

Summarizing above results, for the mechanically alloyed $\text{Fe}_{100-x}\text{Cu}_x$ solid solution, it is likely that the resultant products are mixed by Fe-rich and Cu-rich particles with small grain sizes. The Fe and Cu alloying region is mainly in the coherent interface of both Fe and Cu particles. The mechanism of mechanical alloying is likely to that proposed by Ermakov. (1981) Highly strained small particles with various defects are formed for $\text{Fe}_{100-x}\text{Cu}_x$ supersaturated solid solutions after ball milling. This conclusion is supported by the results of Mossbauer (Li *et al.*, 1995) where the Fe-rich and Cu-rich region were reported, and high-resolution transmission electron microscopy (Huang *et al.*, 1994) where it can be observed the clear particle boundary and the particle sizes are about 20~30Å.

5. Conclusion

With the XAFS technique, we have obtained the quantitative structural parameters of Fe and Cu nearest neighbor coordination for $\text{Fe}_{100-x}\text{Cu}_x$ solid solutions. The local structures around Fe and Cu atoms depend on the initial composition of x value. For the higher Cu concentration ($x \geq 40$), the local structures of Fe and Cu atoms keep a fcc-like structure. For the low Cu concentration ($x \leq 20$), the local structure of Fe and Cu atoms maintains a bcc-like structure. We present that Debye-waller factor σ of fcc Fe-Cu solid solution is larger than that of bcc Fe-Cu one, and the σ of Fe atoms (0.099 Å) is larger than that (0.089 Å) of Cu atoms for

$\text{Fe}_{100-x}\text{Cu}_x$ solid solutions ($x \geq 40$). The results indicate that the mechanically alloyed $\text{Fe}_x\text{Cu}_{100-x}$ is an inhomogeneous supersaturated solid solution, and there are Fe-rich and Cu-rich regions in the MA $\text{Fe}_{100-x}\text{Cu}_x$ solid solutions.

Acknowledgments

We would like to thank National Synchrotron Radiation Laboratory and Beijing Synchrotron Radiation Facility for giving us the beam time for XAFS measurement. This work was supported by "100 people plan" of Chinese Academy of Science and National Natural Science Foundation of China.

References

- Crespo, P., Hernando, A. & Escorial, A.G., (1994). *Phys. Rev. B.* 49, 13227.
- Crespo, P., Hernando, A., Yavari, R., Drbohlav, D., Escorial, A.G., Barandiaran, J.M. & Orue, I., (1993). *Phys. Rev. B.* 48, 7134.
- Doyama, M., Matsui, M., Matsuoka, H., Mitani, S. & Doi, K., (1991). *J. Magn. Magn. Mater.* 93, 374.
- Dubois, J.M., (1988). *J. Less-common Met.* 145, 309.
- Ermakov, A.E., Yivichikov, E.E. & Barinov, V.A., (1981). *Fiz. Met. Metalloved.* 52, 1184.
- Fukunaga, T., M. Mori., Inou, K. & Mizutani, U., (1991). *Mater. Sci. Eng. A.* 134, 863.
- Gaffet, E., Louison C., Harmelin, M. & Faudet, F., (1991). *Mater. Sci. Eng.* A134, 1380.
- Huang, J.Y., He, A.Q., Wu, Y.K., Ye, H.Q., Li, D.X., (1996). *J. Mater. Sci.* 31, 4165.
- Huang, J.Y., Jiang, J.Z., Yasuda, H. & Mori, H., (1998). *Phys. Rev. B.* 58, 11817.
- Huang, J.Y., Wu, Y.K., He, A.Q., Hu, K.Y. and Meng, Q.M., (1994). *J. Chinese Electron Microscopy Society.* 13, 26.
- Keavney, D.J., Storm, D.F., Freeland, J.W., Grigorov, I.L. & Walker, J.C., (1995). *Phys. Rev. Lett.* 74, 4531.
- Koch, C.C., Cavin, O.B., Mckamey, G.G. & Scarbrough, J.O., (1983). *Appl. Phys. Lett.* 43, 1017.
- Li, T., Li, Y.Z., Zhang, Y.H., Gao, C., Wei, S.Q. & Liu W.H., (1995). *Phys. Rev. B.* 52, 1120.
- Miedema, A.R., De, Chatel P.F. & De Boer, F.R., (1980), *Physica B.* 100, 1.
- Sakurai, K., Yamada, Y., Ito, M., Lee, C.H., Fukunaga, T. & Mizutani, U., (1990). *Appl. Phys. Lett.* 57, 2660.
- Sayers, D.E., & Bunker, B.A., (1988). *X-ray Absorption, Principles, Applications, Techniques of EXAFS, SEXAFS and XANES*, P.211, D.C. Koningsberger, & R. Prins, John Wiley and Sons, Inc.
- Schultz, L., (1988). *Mater. Sci. Eng.* 97, 15.
- Schilling, P.J., He, J.-H., Cheng, J. & Ma E., (1996). *Appl. Phys. Lett.* 68, 767.
- Schilling, P.J., He, J.-H., Tittsworth, R.C. & Ma, E., (1999). *Acta Mater.* 47, 2525.
- Shingu, P.H., Ishihara, K.N., Uenishi, K., Kuyama, T., Huang, B. & Nasu, S., (1990). *Solid State Powder Proceeding*, The Minerals Metals and Materials Society, P20.
- Uenishi, K., Kobayashi, F., Nash, S., Hatano, H., Ishihara, K.N. & Shingu, P.H., (1992). *Z. Metallkd.* 83, 132.
- Wan, X.H. & Wei, S.Q., *USTCXAFS Software Package* (May, 1999).
- Wei, S.Q., Oyanagi, H., Wen, C.E., Yang, Y.Z. & Liu, W.H., (1997). *J. Phys. condens. Matter.* 9, 11077.
- Yavari, A.R., Desre, P.J. & Benameur T., (1992). *Phys. Rev. Lett.* 68, 2235.